Molecular Bases of Disease:

Missense Mutation in *APOC3* within the C-terminal Lipid Binding Domain of Human ApoC-III Results in Impaired Assembly and Secretion of Triacylglycerol-rich Very Low Density Lipoproteins: EVIDENCE THAT ApoC-III PLAYS A MAJOR ROLE IN THE FORMATION OF LIPID PRECURSORS WITHIN THE MICROSOMAL LUMEN

Wen Qin, Meenakshi Sundaram, Yuwei Wang, Hu Zhou, Shumei Zhong, Chia-Ching Chang, Sanjay Manhas, Erik F. Yao, Robin J. Parks, Pamela J. McFie, Scot J. Stone, Zhenghui G. Jiang, Congrong Wang, Daniel Figeys, Weiping Jia and Zemin Yao

J. Biol. Chem. 2011, 286:27769-27780.
doi: 10.1074/jbc.M110.203679 originally published online June 15, 2011

THE JOURNAL OF BIOLOGICAL CHEMISTRY VOL. 286, NO. 31, pp. 27769–27780, August 5, 2011

Missense Mutation in *APOC3* within the C-terminal Lipid Binding Domain of Human ApoC-III Results in Impaired Assembly and Secretion of Triacylglycerol-rich Very Low Density Lipoproteins

EVIDENCE THAT ApoC-III PLAYS A MAJOR ROLE IN THE FORMATION OF LIPID PRECURSORS WITHIN THE MICROSOMAL LUMEN[*] [S]

Received for publication, November 16, 2010, and in revised form, June 13, 2011 Published, JBC Papers in Press, June 15, 2011, DOI 10.1074/jbc.M110.203679

Wen Qin[‡1,2], **Meenakshi Sundaram**[§1], **Yuwei Wang**[§], **Hu Zhou**[§], **Shumei Zhong**[§], **Chia-Ching Chang**[¶], **Sanjay Manhas**[§], **Erik F. Yao**[§], **Robin J. Parks**[‖], **Pamela J. McFie**[**], **Scot J. Stone**[**], **Zhenghui G. Jiang**[‡‡], **Congrong Wang**[‡], **Daniel Figeys**[§3], **Weiping Jia**[‡], **and Zemin Yao**[§4]

From the [‡]*Department of Endocrinology and Metabolism, Shanghai Jiao Tong University Affiliated Sixth People's Hospital, Shanghai Diabetes Institute, Shanghai Clinical Center of Diabetes, Shanghai 200233, China, the* [§]*Department of Biochemistry, Microbiology, and Immunology, Ottawa Institute of Systems Biology, University of Ottawa, Ottawa, K1H 8M5 Canada, the* [‖]*Ottawa Hospital Research Institute, Ottawa K1H 8L6, Canada, the* **Department of Biochemistry, University of Saskatchewan, Saskatoon, Saskatchewan S7N 5E5, Canada , the* [¶]*Department of Biological Science and Technology, National Chiao Tung University, Hsinchu 300, Taiwan and Institute of Physics, Academia Sinica, Taipei, Taiwan 11529, and the* [‡‡]*Department of Physiology and Biophysics, Boston University School of Medicine, Boston, Massachusetts 02118-2526*

Hepatic assembly of triacylglycerol (TAG)-rich very low density lipoproteins (VLDL) is achieved through recruitment of bulk TAG (presumably in the form of lipid droplets within the microsomal lumen) into VLDL precursor containing apolipoprotein (apo) B-100. We determined protein/lipid components of lumenal lipid droplets (LLD) in cells expressing recombinant human apoC-III (C3wt) or a mutant form (K58E, C3KE) initially identified in humans that displayed hypotriglyceridemia. Although expression of C3wt markedly stimulated secretion of TAG and apoB-100 as $VLDL_1$, the K58E mutation (located at the C-terminal lipid binding domain) abolished the effect in transfected McA-RH7777 cells and in *apoc3*-null mice. Metabolic labeling studies revealed that accumulation of TAG in LLD was decreased (by 50%) in cells expressing C3KE. A Fat Western lipid protein overlay assay showed drastically reduced lipid binding of the mutant protein. Substituting Lys^{58} with Arg demonstrated that the positive charge at position 58 is crucial for apoC-III binding to lipid and for promoting TAG secretion. On the other hand, substituting both Lys^{58} and Lys^{60} with Glu resulted in almost entire elimination of lipid binding and loss of function in promoting TAG secretion. Thus, the lipid binding domain of apoC-III plays a key role in the formation of LLD for hepatic VLDL assembly and secretion.

Hepatic assembly of very low density lipoproteins (VLDL) rich in triacylglycerol (TAG)[5] is initiated during and after translation and translocation of apolipoprotein (apo) B-100 across the endoplasmic reticulum membrane. The nascent VLDL particle is further enlarged in TAG content through a "second step" lipidation process, where a bulk TAG (presumably present within the microsomal lumen in the form of lipid droplet) is incorporated (1). Although much has been learned about the co- and post-translational lipidation of apoB-100, little is known about the nature or the dynamics of these lumenal lipid droplets (LLD) that are utilized as lipid precursor for VLDL assembly. Early studies with the abetalipoproteinemia gene *MTTP* suggested that the microsomal triglyceride transfer protein (MTP) is required for the partitioning of VLDL lipid precursor, mainly TAG, into the microsomal lumen in mouse liver (2), cultured murine primary hepatocytes (3), and the rat hepatoma McA-RH7777 cells (4). Thus, inactivation of MTP in the liver cells was associated with lack of LLD and invariably resulted in diminished assembly and secretion of VLDL. Recent proteomic and lipid characterization of LLD isolated from murine liver microsomes has shown that these lipid-rich entities are devoid of apoB but contain proteins such as TAG hydrolase, carboxylesterase 1, MTP, and apoE (5). Working with McA-RH7777 cells stably expressing recombinant human apoC-III, we have obtained evidence for the presence of a metabolically active TAG-rich entity within the microsomal lumen, which has a buoyant density resembling that of intermediate density lipoproteins (IDL) and low density lipoproteins (LDL)

* This work was supported by the Heart and Stroke Foundation of Ontario (NA-7026 (to Z. Y.), China-Canada Health Research Initiative Grants CCI 92211 (to Z. Y.), and 30811120437 (to W. J.), and by the J.-Louis Lévesque Foundation (to D. F.).

[S] The on-line version of this article (available at http://www.jbc.org) contains supplemental Tables 1–3 and Fig. S1.

[1] Both authors contributed equally to this work.

[2] Recipient of Special Funding for Visiting Doctoral Students Program from Shanghai Jiao Tong University.

[3] The Tier I Canada Research Chair in Proteomics and Systems Biology.

[4] To whom correspondence should be addressed: 451 Smyth Rd., Dept. of Biochemistry, Microbiology and Immunology, University of Ottawa, Ottawa, ON, K1H 8M5 Canada. E-mail: zyao@uottawa.ca.

[5] The abbreviations used are: TAG, triacylglycerol; LLD, lumenal lipid droplet; MTP, microsomal triglyceride transfer protein; IDL, intermediate density lipoprotein; PC, phosphatidylcholine; DAG, diacylglycerol; PE, phosphatidylethanolamine; SPM, sphingomyelins; P407, Poloxamer 407; DGAT, diacylglycerol acyltransferase; Tricine, *N*-[2-hydroxy-1,1-bis(hydroxymethyl) ethyl]glycine.

(6). Interfering with the second step lipidation, either via treatment with brefeldin A or by expression of a loss-of-function human apoC-III mutant A23T, resulted in accumulation of metabolically labeled TAG in the form of LLD in microsomes (6). These results suggest that human apoC-III may play a functional role in the formation of the VLDL lipid precursors in the liver.

Apolipoprotein C-III is a small (79 amino acids) protein that comprises 40% of the protein mass of plasma VLDL and is also a component of HDL (7, 8). Mouse and human studies have demonstrated a strong positive correlation between plasma apoC-III and TAG concentrations (9) that is attributable to the inhibitory effect of apoC-III exerted on the TAG hydrolysis catalyzed by lipoprotein lipase (10) and the clearance of TAG-rich lipoproteins via receptor-mediated endocytosis (11). Recently, *in vivo* (12, 13) and *in vitro* (6, 14) experimental evidence has suggested that the apoC-III level is positively linked to hepatic VLDL production, presumably through enhanced assembly and secretion of TAG-rich $VLDL_1$.

The structural elements within apoC-III responsible for promoting TAG-rich $VLDL_1$ secretion remain to be determined. *In vitro* studies suggested that the lipid binding activity of apoC-III resides within the C-terminal region encompassing amino acid residues 41–79 (15). Thus, mutation at the N-terminal region (*e.g.* A23T) does not appear to affect apoC-III binding to lipid (6). In the current work we tested the effect of the naturally occurring mutation K58E (16) that is located within the lipid binding domain of apoC-III. Clinical data showed that the heterozygous K58E carriers had increased HDL (>95th percentiles of sex matched controls) and lowered VLDL as well as lowered VLDL-apoC-III (15% of normal) (16). The present data have demonstrated that the K58E mutation entirely abolished the apoC-III stimulatory effect on assembly and secretion of TAG-rich VLDL and resulted in markedly retarded accumulation of LLD in transfected cells. Thus, the lipid binding domain of apoC-III plays a key role in the formation of LLD utilized for VLDL assembly and secretion under lipid-rich conditions.

EXPERIMENTAL PROCEDURES

Materials—Medium and reagents used for cell culture studies were obtained from Invitrogen. [^{35}S]Methionine/cysteine (1000 Ci/mmol) was obtained from PerkinElmer Life Sciences, and protein A-Sepharose^{TM} CL-4B beads, horseradish peroxidase-linked anti-mouse, and anti-rabbit IgG antibodies were obtained from GE Healthcare. [2-^{3}H]Glycerol (9.6 Ci/mmol) was obtained from American Radiolabeled Chemicals (St. Louis, MO), and brefeldin A and horseradish peroxidase-linked anti-goat antibody were obtained from Sigma. Oleate, TAG, and phospholipid standards were from Avanti Polar Lipids (Alabaster, AL). Antibody against human apoC-III (used for Western blot analysis) was obtained from Academy Biomedical Co., Inc. (Houston, TX). Polyclonal anti-mouse apoA-I and anti-mouse apoE antisera were obtained from BioDesign International (Saco, ME). Polyclonal antisera against rat VLDL (used for immunoprecipitation of apoB-100) or human apoC-III (used for immunoprecipitation of apoC-III) were generated in our laboratory. Protease inhibitor mixture and chemiluminescent substrates were obtained from Roche Diagnostics. Poloxamer 407 (P407) was a gift from BASF Corp. (Florham Park, NJ).

Preparation of Expression Plasmids and Transfection—The wild type human apoC-III (C3wt) expression plasmid (14) was used to generate cDNAs with site specific mutations such as K58E (C3KE), K58R (C3KR), K58E/K60E, and K58E/K60R within the coding region of human apoC-III cDNA using appropriate forward and reverse primers and QuikChange^{TM} mutagenesis kit (Stratagene, Ann Arbor, MI). The coding sequences of all cDNA constructs were verified by sequencing. Sequences of the mutagenesis and sequencing primers are listed in supplemental Table 1. Stably transfected McA-RH7777 cells expressing wild type or the respective mutant apoC-III were generated as described previously (14). The cells were maintained in Dulbecco's modified Eagle's medium (DMEM) containing 10% fetal bovine serum, 10% horse serum, and 200 μg/ml G418.

Metabolic Labeling of Lipids—Cells (~1.8×10^6 cells/60-mm dish, in triplicate) were labeled with [^{3}H]glycerol (5 μCi/ml) in DMEM supplemented with 20% FBS and 0.4-mm oleate for up to 2 h. At the end of labeling, lipids were extracted from cells and conditioned media for lipid analysis as described previously (14).

Subcellular Fractionation—Cells (~6×10^6 cells/100-mm dish, in duplicate) were labeled with [^{3}H]glycerol (20 μCi/ml) in DMEM supplemented with 20% FBS and 0.4 mM oleate for 30, 60, and 120 min. At each time point, media were collected for lipid analysis. Cells were harvested in 2 ml of Tris-sucrose buffer (10 mM Tris-HCl, pH 7.4, and 250 mM sucrose) that was supplemented with protease inhibitor mixture and homogenized in a ball-bearing homogenizer (20 passages). The post-nuclear supernatant was obtained by centrifugation (1000 × *g*, 4 °C, 10 min) and was loaded into a quick-seal centrifuge tube. Cytosol and total microsomes were separated by centrifugation using a Beckman TLA-100.3 rotor (500,000 × *g*, 4 °C, 30 min). The total microsomes were rinsed twice with Tris-sucrose buffer to minimize cytosol contamination. The lumenal contents were released from total microsomes with 0.1 M sodium carbonate, pH 11.3, by gentle mixing using a nutator for 30 min at room temperature. The lumenal contents were separated from microsomal membranes by ultracentrifugation (500,000 × *g*, 4 °C, 30 min). Lumenal contents were further subjected to cumulative rate floatation ultracentrifugation (4). Lipids were extracted from subcellular fractions (*i.e.* cytosol, total microsomes, microsomal lumen, and membrane), lumenal lipoprotein fractions were separated by TLC, and the radioactivity associated with [^{3}H]TAG, [^{3}H]DAG, and [^{3}H]phosphatidylcholine (PC) was quantified by scintillating counting as previously described (14).

Lipid Pulse-chase Experiments—Cells (~ 1.8×10^6 cells/60-mm dish, in triplicates) were labeled with [^{3}H]glycerol (5 μCi/ml) in DMEM supplemented with 20% FBS and 0.4 mM oleate for 1 h. Increasing concentrations of triacsin C (0–40 μM) were included in the labeling media to determine the optimum condition for blocking TAG synthesis. In subsequent experiments, 40 μM triacsin C was included in the chase media (DMEM supplemented with 20% FBS, 0.4 mM oleate) for up to 8 h. Lipids were extracted from cell and media at the indicated

chase time and analyzed as described previously (14). The total radioactivity (cell and media) associated with [^{3}H]DAG, [^{3}H]TAG, and [^{3}H]PC at each chase time was plotted as the percentage of initial counts (*i.e.* end of 1 h of labeling in the absence of triacsin C).

Metabolic Labeling of Proteins—Cells (100-mm dishes) were labeled with [^{35}S]methionine/cysteine (100 μCi/ml) for 60 and 120 min in 5 ml of methionine/cysteine-free DMEM supplemented with 20% FBS and 0.4 mM oleate. Cells were harvested and homogenized using ball-bearing homogenizer. Microsomes were obtained by ultracentrifugation, and the lumenal contents were released by treatment with Na_2CO_3 as described above. The lumenal contents were separated from the microsome membranes as described above, and lumenal contents were further subjected to cumulative rate floatation ultracentrifugation. The ^{35}S-labeled apoB-100 and apoC-III proteins were immunoprecipitated from each fraction using appropriate antibodies and resolved by SDS-PAGE followed by fluorography. Radioactivity associated with these apolipoproteins was determined by scintillation counting as previously described (14).

Lipoprotein Fractionation—Cells (100-mm dishes) were labeled for 2 h with [^{35}S]methionine/cysteine (100 μCi/ml) in methionine/cysteine-free DMEM supplemented with 20% FBS and 0.4 mM oleate. The lipoproteins secreted into the conditioned media were fractionated by cumulative rate floatation ultracentrifugation to separate $VLDL_1$ ($S_f > 100$) and $VLDL_2$ (S_f 20–100) from other dense lipoproteins (4). In some experiments where better resolution for HDL fractionations was desired, the conditioned media were fractionated by sucrose density gradient ultracentrifugation (17). To this end, the media (4 ml) were centrifuged at 1000 rpm for 3 min to pellet cell debris. The supernatant was transferred to another tube, and the volume was adjusted to 5 ml with PBS. Sucrose density gradient was formed in 12-ml Ultra-Clear centrifuge tubes (Beckman Coulter) by layering from the bottom of the tube with 2 ml of 54% sucrose, 2 ml of 25% sucrose, 5 ml of sample in 12.5% sucrose, and 3 ml of PBS. The gradients were centrifuged at 35,000 rpm in a Beckman SW41Ti rotor for 65 h at 12 °C. Twelve 1-ml fractions were collected from the top of the tube, and the HDL apolipoproteins (*e.g.* apoE, and apoA-I) from each fraction were recovered by immunoprecipitation using respective polyclonal antibodies and analyzed by SDS-PAGE followed by fluorography. Radioactivity associated with ^{35}S-labeled apolipoproteins or ^{3}H-labeled lipids was quantified by scintillation counting.

For lipid labeling, the cells (100-mm dish) were labeled with [^{3}H]glycerol (5 μCi/ml) in DMEM for 2 h. The ^{3}H-labeled lipids were extracted from each fraction and separated by TLC as described above. Radioactivity associated with ^{3}H-labeled lipids was determined by scintillation counting.

Analysis of Medium Lipoproteins by Size Exclusion Chromatography—Cells (100 mM dishes) were cultured for 2 h in 3 ml of DMEM supplemented with 2% FBS and 0.4 mM oleate. The conditioned media were concentrated centrifugally to 80 μl using Amicon Ultra 0.5-ml (M_r cut-off, 3000) filters (Millipore Corp., Billerica, MA), and a 65-μl aliquot was applied to a Superose 6 HR 10/30 column (Amersham Biosciences) on a HPLC system (Gilson, Middleton, WI). Samples were eluted with a buffer containing 150 mM NaCl, 10 mM Na_2HPO_4, 100 μM EDTA, pH 7.5, at a flow rate of 0.5 ml/min. Forty 0.5-ml fractions were collected, and lipoproteins present in fractions from 14–40 were concentrated using hydrated fumed silica (Cab-O-Sil) as previously described (18). The silica bound proteins were eluted into 100 μl of SDS-PAGE sample buffer (8 M urea, 2% SDS, 10% β-mercaptoethanol), resolved by SDS-PAGE (12% gel) using the Tris-Tricine-SDS running buffer system, and detected for apoC-III by immunoblot analysis using anti-human apoC-III antibody as previously described (14). Elution profiling of VLDL (fractions 14–17), IDL/LDL (fractions 18 through 24), and HDL plus lipid-free proteins (fractions 25–40) was calibrated using mouse serum as previously reported (19).

Liquid Chromatography-MS/MS and Data Analysis of Proteins Associated with Lumenal Lipid Droplet—The LLDs with buoyant density resembling IDL/LDL were isolated from the microsomal lumen of cells expressing apoC-III as described previously (6). The LLD-associated proteins were resolved by SDS-PAGE (3–15% gel), and in-gel digestion of the resolved protein was performed as previously described (20). The resulting peptides from the gel bands were resolved in 5% formic acid and loaded on a 200-μm × 50-mm fused silica precolumn packed in-house with 5 cm of 5 μm Magic C18 AQ resins (5 μm, 200 Å; Michrom Bioresources, Auburn, CA) using a 1100 micro-HPLC system (Agilent Technologies, Santa Clara, CA). Following a desalting step, the flow was split, and peptides were eluted through a second 75-μm × 50-mm column packed with the same beads at ~200 nl/min. The peptides were eluted using a 2-h gradient (5–80% acetonitrile with 0.1% formic acid) into an ESI LTQ linear ion trap mass spectrometer (Thermo Electron, Waltham, MA). MS/MS spectra were acquired in a data-dependent acquisition mode that automatically selected and fragmented the 10 most intense peaks from each mass spectrum generated. The acquired MS/MS spectra were searched against the rat International Protein Index protein sequence data base (Version 3.52, 39,906 protein sequences; European Bioinformatics Institute) augmented with the reversed sequence of each entry in the forward data base. Mascot 2.2.02 (Matrix Science) was used to search the protein sequence data base. The precursor and fragment mass tolerances for the LTQ data were set at 2.0 and 0.8 Da, respectively. Mascot cutoff scores were set to 30. Peptides ranked with a probability based Mowse (expect) $p < 0.05$ were accepted. The false positive rate was controlled at <1%.

Fat Western Lipid Protein Overlay Assay—The apoC-III-lipid binding assays were performed according to previously published protocol (21) with modifications. Briefly, various amounts (5–100 μg) of phospholipids and neutral lipids were spotted on Trans-Blot nitrocellulose membranes (Bio-Rad). Blots were blocked with phosphate-buffered saline containing 3% (w/v) fatty acid-free BSA and incubated at 4 °C for 12 h with equal amounts of apoC-III in conditioned media (collected from 100-mm dishes of cells cultured for 16 h in serum-free media). After washing with PBS and blocked with 5% fat-free milk in blotto, the blots were incubated with goat anti-human apoC-III antibody (1:2000) overnight at 4 °C. Blots were washed

with PBS and incubated in HRP-conjugated anti-goat IgG secondary antibody (1:10,000) for 1 h at room temperature followed by washing with PBS.

The apoC-III bound to spotted lipids was visualized by enhanced chemiluminescence as per the supplier's (Roche Diagnostics) instructions, and the intensity of each spot was quantified by scanning densitometry. The densitometry data were fitted into the Hill equation, $\theta = [L]^n/(K_A{}^n + [L]^n)$, by the least square fitting method to calculate apoC-III lipid binding kinetics. In the Hill equation, θ represents the relative amount of apoC-III that binds to lipids, L is the amount of lipid (in moles), K_{1a} is the amount of lipid to which apoC-III displayed half-maximum binding, which is also the microscopic dissociation constant, and n is the Hill coefficient.

Real-time RT-PCR—Isolation of RNA from cells, reverse transcription, and relative mRNA concentration determination by real-time RT-PCR were performed as described previously (14). Cyclophilin A was used as the RT-PCR control. The primers used for RT-PCR were obtained from Sigma, and sequences of the primers are listed in supplemental Table 2.

In Vivo Hepatic VLDL Production Assay—*apoc3*-null mice (B6.129-*apoc3*$_{tm1Unc}$/J) obtained from The Jackson Laboratory (Bar Harbor, ME) were maintained and bred at the University of Ottawa animal care facility according to approved protocols. Male mice (8–12 weeks old) were fed with high fat diet (TD.88137, Harlan Laboratories, Madison, WI) for 2 weeks and injected with adenovirus encoding either wild type human apoC-III (adv-C3wt) or the K58E mutant (adv-C3KE) via tail vein (1×10^9 plaque-forming units/mouse). Two days after infection, mice were fasted for 16 h. Blood samples were collected via saphenous vein to determine expression of the recombinant apoC-III. Accumulation of newly synthesized apoB100 and apoB48 in the plasma was determined by injection of P407 (1 mg/g of body weight) to block VLDL lipolysis, and plasma samples were collected at 1 and 2 h after P407 injection. Plasma lipoproteins were separated by cumulative rate flotation centrifugation. An aliquot (100 μl) of each lipoprotein fraction was mixed with 150 μl of the TAG reagent (Infinity^{TM} Triglycerides, Thermo Scientific, Middletown, VA). Samples were incubated at 37 °C for 15 min, and the absorbance was measured at 520 nm. The apoB-100 and apoB-48 mass in TAG-rich lipoprotein fractions was semiquantified by immunoblotting after SDS-PAGE.

Histology of the Liver—The livers were fixed in 4% paraformaldehyde for 24 h after, sliced into 1-mm specimens, and treated with 1% osmium tetroxide (in PBS) for 1 h. The specimens were washed with PBS (10 min, two times), placed in 70% alcohol, and processed for paraffin embedding using ATP1 automatic histoprocessor (Triangular Biomedical Sciences, Durham, NC). Paraffin sections (2.5-μm thickness) were obtained, dried, deparaffinized, and stained with 1% nuclear fast red for 5 min. Sections were dehydrated in alcohol, cleared with toluene, and mounted on glass slides using Permount (Fisher). Slides were scanned using Zeiss Mirax Midi microscope scanner, and the images were analyzed using Mirax Viewer software (Carl Zeiss Canada Ltd., Toronto, Canada).

Quantification of TAG Mass in the Liver—The livers (100–120 mg by weight) were homogenized using Polytron Homogenizer (Kinematica AG, PT 10-35) in chloroform:methanol (2:1, v/v), and the homogenate was mixed overnight on a shaker. After centrifugation, the organic solvent was recovered, dried under N_2 (60 °C water bath), resuspended in 6 ml of chloroform:methanol (2:1, v/v), and mixed with 1.2 ml of H_2SO_4 (0.05%, v/v). The aqueous and organic solvent phases were separated by centrifugation, and an aliquot (250 μl) of the solvent phase was dried under N_2 (60 °C) and resuspended in 2 ml of chloroform and 1% Triton X-100. The samples were dried under N_2 (60 °C) and solubilized in 1 ml of distilled water. An aliquot (10 μl) of the sample was diluted 5-fold and mixed with 150 μl of TAG reagent to quantify TAG as described above.

Other Assays—The *in vitro* diacylglycerol acyltransferase (DGAT) activity assay in cell lysate was determined by measuring the formation of [^{14}C]TAG from [^{14}C]oleoyl CoA as described previously (22). Briefly, cells were lysed by passing the cells suspended in lysis buffer (50 mM Tris, pH 7.6, 250 mM sucrose) through a 27-gauge needle 10–15 times. Cell debris was pelleted by centrifugation 600 $\times$ *g* for 5 min. Supernatant lysate was used for DGAT assays. The reaction contained 100 mM Tris-HCl, pH 7.5, 20 or 100 mM $MgCl_2$, 0.625 mg/ml BSA, 200 mM 1,2-dioleoylglycerol, 25 μM [^{14}C]oleoyl-CoA (18 mCi/mmol), and 50 mg of protein (cell lysate) in a final volume of 200 μl. The assay was incubated at 37 °C for 10 min. The reaction was terminated by the addition of chloroform:methanol (2:1 v:v) followed by 800 μl of H_2O. Lipids were extracted and separated by TLC using hexane:ethyl ether:acetic acid (80:20:1 v:v:v) as a solvent system. Radioactivity in the [^{14}C]TAG band was quantified by liquid scintillation counting.

The *in vitro* MTP activity in the cell lysate of apoC3wt or apoC3KE cells was determined as described previously (23, 24). Protein concentration was quantified by the Bradford method (25).

RESULTS

K58E Is a Loss-of-function Mutation—The human apoC-III is composed of six α-helices (26) of which helix 5, where the K58E mutation resides, assumes a typical type A amphipathic configuration (Fig. 1*A*). In this structure, Lys^{58} and Lys^{60} situate at the plane of water-lipid interface, with hydrophobic residues on one side of the helix and acidic residues on the opposite side (27). Intuitively, substitution of Lys^{58} with Glu would be expected to destroy the type A amphipathic configuration of helix 5 and impair lipid binding. To determine the effect of K58E mutation, we contrasted expression of the mutant with that of wild type apoC-III on VLDL-TAG secretion. From three stable clones expressing different levels of the mutant apoC-III (designated *C3KE*; Fig. 1*B*), secretion of [^{3}H]glycerol-labeled TAG was invariably decreased as compared with wild type apoC-III expressing cells (C3wt) regardless of the level of mutant expression (Fig. 1*C*). Fractionation of lipoproteins secreted from C3KE or C3wt cells showed that whereas [^{3}H]TAG secretion as $VLDL_1$ was markedly stimulated by C3wt expression, this stimulatory effect was lost in C3KE-expressing cells (Fig. 1*D*). The lack of a stimulatory effect of C3KE on $VLDL_1$ secretion was further confirmed by metabolic labeling of apoB-100. From C3wt cells, the secreted ^{35}S-apoB-100 was predominately associated with VLDL (*i.e.* $VLDL_1$ and $VLDL_2$),

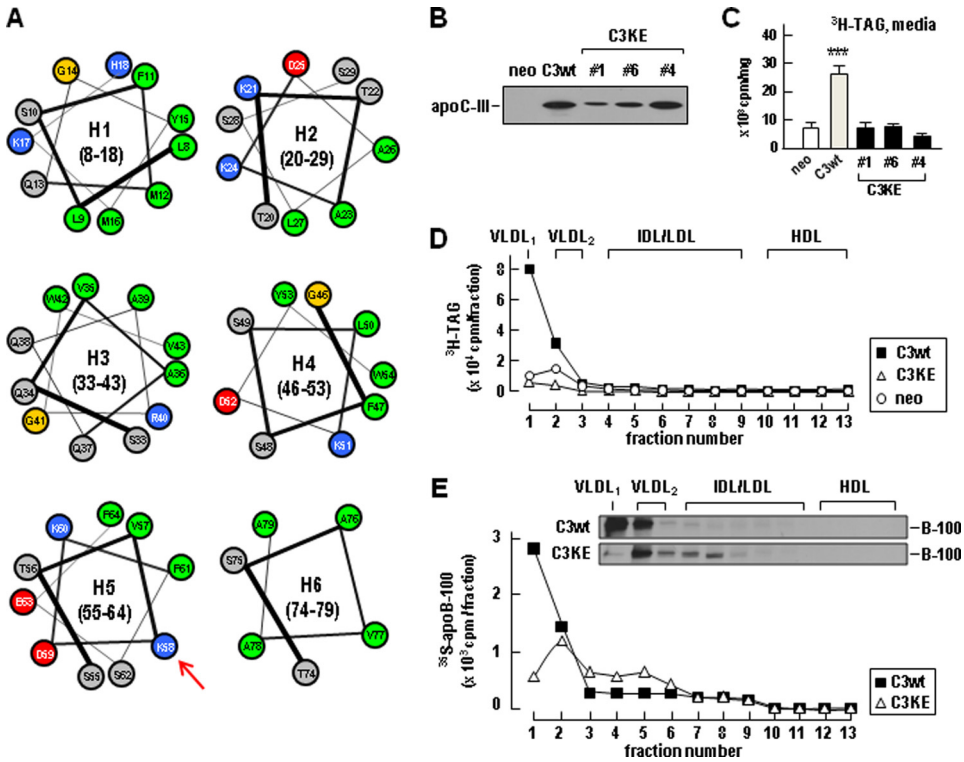

FIGURE 1. **The K58E is a loss-of-function mutation that abolished TAG-rich VLDL$_1$ secretion.** *A*, the six α-helices of human apoC-III in helix wheel diagram are shown. The secondary structure assignment was based on the apoC-III structure (PDB ID 2jq3) in SDS-bound state as determined by NMR (26). Hydrophobic residues are denoted in *green*, acidic residues are in *red*, basic residues are in *blue*, hydrophilic residues are in *gray*, and Lys^{58} is marked with a *red arrow*. *B*, shown is an immunoblot of recombinant human apoC-III expressed in McA-RH7777 cells. *C3wt*, wild type apoC-III; *C3KE*, the K58E variant. *C*, cells (1.8×10^6 cells/60 mM dish, in triplicate) were labeled with [^{3}H]glycerol (5 μCi/ml) for 2 h in DMEM containing 20% FBS and 0.4 mM oleate. Lipids were extracted from media and cells at the end of labeling and resolved by TLC. Radioactivity associated with [^{3}H]TAG was quantified by scintillation counting. Radioactivity associated with the [^{3}H]TAG in the media is shown. ***, $p < 0.001$ (Student's *t* test of C3wt *versus neo* or C3KE *versus neo*; $n = 3$). *D*, cells were labeled with [^{3}H]glycerol for 2 h in the presence of 20% serum and 0.4 mM oleate. At the end of labeling, media were subjected to cumulative rate flotation ultracentrifugation. Lipids were extracted from each fraction and separated by TLC. Radioactivity associated with [^{3}H]TAG was quantified by scintillation counting. *E*, cells were labeled with [^{35}S]methionine/cysteine for 2 h in the presence of 20% serum and 0.4 mM oleate. At the end of labeling, media were subjected to cumulative rate flotation ultracentrifugation. ApoB-100 was recovered from each fraction by immunoprecipitation and resolved by SDS-PAGE and visualized by fluorography (*top two panels*). Radioactivity associated with ^{35}S-apoB100 was quantified by scintillation counting and plotted (*bottom panel*).

whereas from C3KE cells the ^{35}S-apoB-100 was absent in VLDL$_1$ and present in VLDL$_2$ and IDL/LDL fractions (Fig. 1*E*, fluorograms for ^{35}S-apoB-100 are shown in the *insets*). Together, these results are the first indication that K58E is a loss-of-function mutation that abolishes the stimulatory effect of apoC-III on TAG-rich VLDL$_1$ secretion under lipid-rich conditions.

Determination of lipoprotein-association of secreted ^{35}S-apoC-III by density ultracentrifugation showed that C3wt was associated with VLDL in addition to HDL-like fractions, whereas C3KE mutant was present only in HDL-like fractions and the bottom fractions (Fig. 2*A*). To rule out that the lack of C3KE association with VLDL was not attributable to ultracentrifugation, we fractionated the conditioned media using FPLC that minimizes detachment of apoC-III from lipoproteins. The FPLC profiling showed that although the wild type apoC-III was predominantly associated with VLDL fractions, the C3KE mutant was devoid in VLDL fractions and eluted almost exclusively in HDL and lipoprotein-free fractions (Fig. 2*B*). These results together with the density ultracentrifugation data (Fig. 1*E*),indicate that the K58E mutation resulted in decreased binding of apoC-III to VLDL (*i.e.* VLDL$_1$ or VLDL$_2$).

It was reported that the heterozygote carriers of the K58E mutation had increased HDL in the face of decreased VLDL (16). Thus, we also determined the effect of C3wt or C3KE expression on the secretion of apoA-I and apoE, two HDL-associated apolipoproteins. To this end, the conditioned media were fractionated by sucrose density gradient ultracentrifugation to better resolve the HDL particles (ranging from $d = 1.07$ through $d = 1.24$ g/ml). Secretion and density distribution of ^{35}S-apoA-I from C3KE cells was comparable with that from C3wt cells (Fig. 2*C*). Likewise, secretion of ^{35}S-apoE from C3KE cells did not show major changes as compared with that from C3wt cells either under conditions of minus or plus heparin (to prevent reuptake of apoE-containing lipoproteins) (Fig. 2, *D* and *E*). Thus, the current cell culture model does not offer evidence for the hyperalphalipoproteinemia phenotype observed in heterozygotes carriers of the K58E mutation (16).

However, the hypotriglyceridemia phenotype could be recapitulated in *apoc3*-null mice infected with adenovirus encoding either C3wt or C3KE mutant (Fig. 3*A*). Infection of the mice, fed with a high fat diet for 2 weeks, with C3wt virus (adv-C3wt) resulted in marked accumulation of apoB-100 and apoB-48 in VLDL$_1$ fractions under conditions where lipolysis was inhibited (*i.e.* with P407) (Fig. 3*B*). In contrast, expression of C3KE mutant (adv-C3KE) under identical conditions failed to stimulate VLDL$_1$ production (Fig. 3*C*). Quantification of TAG mass in the fractionated medium

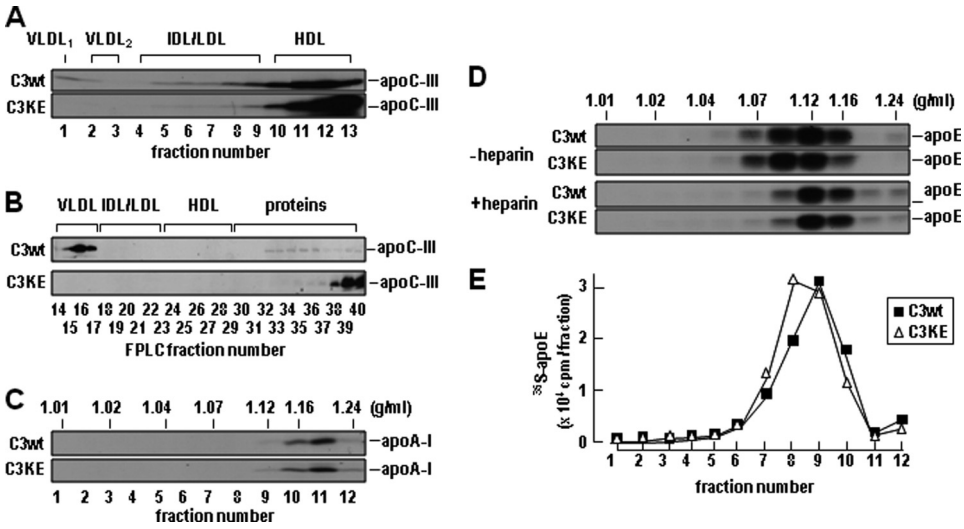

FIGURE 2. **Impaired $VLDL_1$-apoC-III secretion from C3KE cells.** *A*, C3wt and C3KE cells were labeled with [^{35}S]methionine/cysteine for 2 h in the presence of 20% serum and 0.4 mM oleate. The conditioned media were fractionated by cumulative rate flotation ultracentrifugation, and immunoprecipitated ^{35}S-apoC-III was resolved by SDS-PAGE and visualized by fluorography. *B*, conditioned media were fractionated by size exclusion chromatography using FPLC and apoC-III in fractions 14–40 were recovered by immunoprecipitation, resolved by SDS-PAGE, and visualized by immunoblotting. *C*, cells were treated as in *A*, and the conditioned media were subjected to sucrose density gradient ultracentrifugation. The immunoprecipitated ^{35}S-apoA-I proteins were resolved by SDS-PAGE and visualized by fluorography. *D*, the ^{35}S-labeled conditioned media (−*heparin*, *top panels* or +*heparin* (100 units/ml), *bottom panels*) were subjected to sucrose density gradient ultracentrifugation, and the immunoprecipitated apoE proteins were resolved by SDS-PAGE and visualized by fluorography. *E*, the radioactivity associated with ^{35}S-apoE was quantified using scintillation counter (only data were obtained under minus heparin conditions are shown). The density (g/ml) of each fraction, which is the mean value of seven density gradients determined gravimetrically, is shown on *top* of the fluorograms in *panels C* and *D*. Repetition of the experiments yielded similar results.

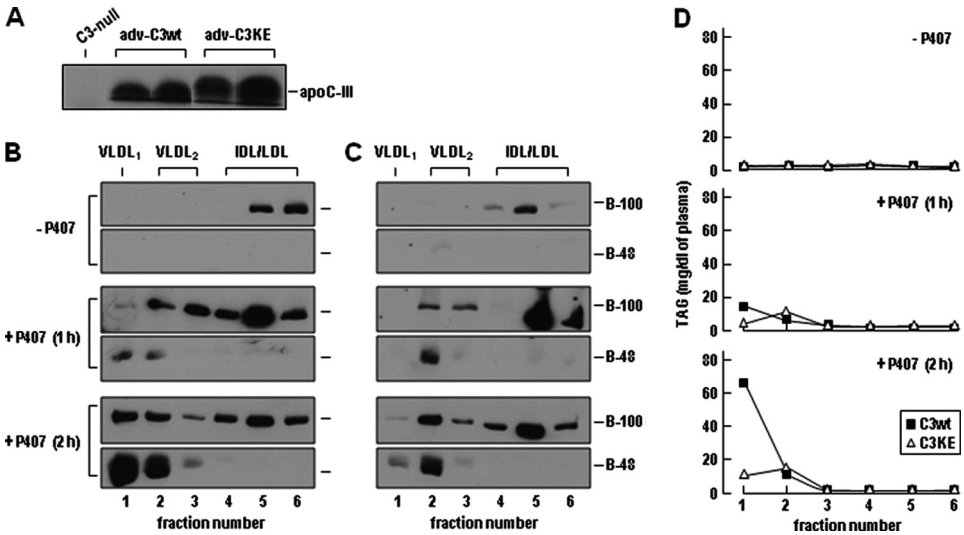

FIGURE 3. **Hepatic $VLDL_1$ production was impaired in *apoc3*-null mice expressing apoC3KE protein.** The *apoc3*-null mice (10 weeks old) fed with a high fat diet for 2 weeks were infected with adenovirus encoding C3wt or C3KE. Three days after infection, mice were fasted for 16 h. Blood samples were collected before or 1 and 2 h after P407 injection. *A*, immunoblots of apoC-III in plasma of infected mice are shown. *B* and *C*, shown are immunoblots of apoB-100 and apoB48 in fractionated plasma lipoproteins (only the top six fractions of cumulative rate flotation centrifugation are shown). The plasma samples were pooled from three mice infected with adv-C3wt (*B*) or adv-C3KE (*C*). Samples were collected before (*top two panels*) and 1 h (*middle two panels*) or 2 h (*bottom two panels*) after P407 injection. *D*, TAG mass in the top six fractions of cumulative rate flotation centrifugation (*i.e.* $VLDL_1$, $VLDL_2$, and IDL/LDL) of plasma samples pooled from three adv-C3wt- and three adv-C3KE-infected mice before (*top panel*), 1 h (*middle panel*), or 2 h (*bottom panel*) after P407 injection.

lipoproteins showed that the vast majority of TAG was associated with $VLDL_1$ (Fig. 3*D*), and the $VLDL_1$-TAG accumulated in the plasma of adv-C3wt-infected mice was >4-fold higher than that of adv-C3KE-infected mice (Fig. 3*D*). There was no significant difference in TAG mass associated with $VLDL_2$ or IDL/LDL fractions between adv-C3wt- and adv-C3KE-infected mice. Thus, the K58E mutation specifically impaired $VLDL_1$ production in both the McA-RH7777 cell culture model and the *apoc3*-null mouse model.

Impaired Lumenal Lipid Droplets Formation in Cells Expressing C3KE Mutant—Our previous studies with McA-RH7777 cells stably expressing human apoC-III have suggested that LLD presented in the microsomes (with buoyant density resembling IDL/LDL) may represent the bulk TAG precursor utilized for $VLDL_1$ assembly/secretion (14). Analysis of proteins associated with LLD by liquid chromatography-MS/MS revealed that the LLD fractions were devoid of apoB-100 and contained apoC-III and apoE in addition to 40 other proteins,

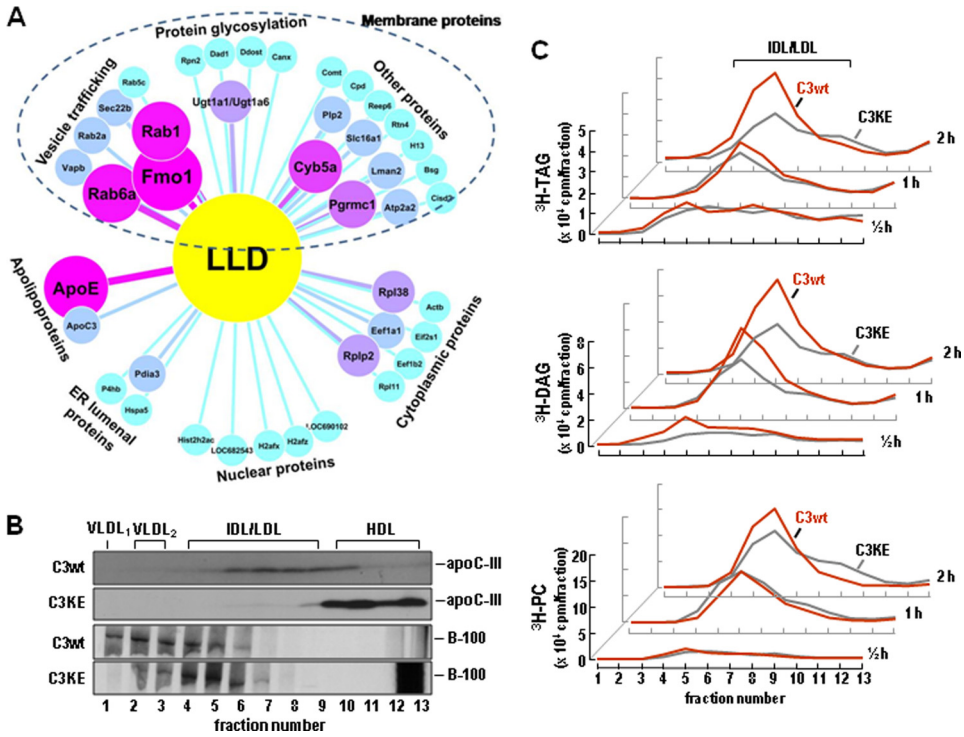

FIGURE 4. **Impaired LLD formation in C3KE cells.** *A*, shown is a proteomics analysis of LLD-associated proteins. C3wt cells were cultured in DMEM supplemented with 20% serum and 0.4 mM oleate. The cells were homogenized to isolate the microsomes, and the lumenal contents were released from the microsomes by Na_2CO_3 treatment. The content was fractionated by cumulative rate flotation centrifugation to obtain LLD fractions, and the identity of the LLD-associated proteins was determined by liquid chromatography-MS/MS as described under "Experimental Procedures." The identified proteins are visualized using Cytoscape software (Version 2.6.0) (34). The line width, size, and color intensity of each individual protein is related to its identified peptides. The detailed information of each identified protein is shown in supplemental Table 3. *B*, apoC-III and apoB-100 distribution within microsomal lumen is shown. C3wt and C3KE cells were labeled with [^{35}S]methionine/cysteine for 60 min in the presence of 20% serum and 0.4 mM oleate. Microsomal content was fractionated as in *A*. The ^{35}S-apoC-III (*top two panels*) or ^{35}S-apoB-100 (*bottom two panels*) in each fraction was recovered by immunoprecipitation, resolved by SDS-PAGE, and visualized by fluorography. *C*, C3wt and C3KE cells ($\sim 6 \times 10^6$ cells/100-mm dish, in duplicates) were labeled with [^{3}H]glycerol (20 μCi/ml) in DMEM supplemented with 20% FBS and 0.4 mM oleate for 0.5, 1, and 2 h. At the end of labeling, cells from two dishes were combined, and lumenal content was isolated from the microsomes followed by fractionation as in *A*. Lipids were extracted from each fraction and resolved by TLC. Radioactivity associated with [^{3}H]TAG (*top*), [^{3}H]DAG (*middle*), and [^{3}H]PC (*bottom*) was quantified and plotted.

including those involved in vesicle trafficking, protein glycosylation, endoplasmic reticulum lumenal proteins, and some proteins normally present in nucleus or cytoplasm (Fig. 4*A*). Whether or not all of these membrane or cytoplasmic proteins are functional components of LLD remains to be determined experimentally (see supplemental Table 3).

Determination of metabolically labeled apoC-III distribution within the microsomal lumen confirmed that apoC-III indeed was a component of LLD. The majority of lumenal ^{35}S-C3wt was associated with the isolated LLD fractions, whereas ^{35}S-C3KE was unable to bind to LLD in the microsomes and, rather, was sedimented to HDL and the bottom fractions after ultracentrifugation (Fig. 4*B*, *top two panels*). Determination of lumenal ^{35}S-apoB-100 distribution under the same conditions showed that although apoB-100 was readily detectable in the $VLDL_1$ fractions in C3wt cells, it was mainly associated with IDL/LDL fractions in C3KE cells (Fig. 4*B*, *bottom two panels*), These results suggest that the loss of C3KE binding to LLD was associated with decreased $VLDL_1$ assembly within the microsomal lumen.

The reduced lipid binding activity of C3KE mutant was also associated with impaired accumulation of metabolically labeled lipids in the LLD fractions. Thus, although accumulation of [^{3}H]glycerol-labeled TAG and PC in LLD fractions was readily detectable in C3wt cells, the magnitude of LLD-associated [^{3}H]TAG in C3KE cells was markedly reduced (by >2-fold) (Fig. 4*C*, *top panel*). Similarly decreased accumulation of LLD-associated [^{3}H]DAG in C3KE cells was also observed (Fig. 4*C*, *middle panel*). The effect of K58E mutation on LLD-associated [^{3}H]PC was less pronounced (Fig. 4*C*, *bottom panel*). These results, in accordance with previous data (14), suggest a strong correlation between formation of LLD-associated [^{3}H]TAG and assembly/secretion of $VLDL_1$-[^{3}H]TAG under lipid-rich conditions.

Lipid Binding of ApoC-III Is Compromised by K58E Mutation—The above results suggested a close link between the dynamic biosynthesis of LLD and VLDL-TAG secretion, the establishment of which is facilitated by apoC-III. To gain an insight into mechanism by which apoC-III facilitates LLD formation, we compared the binding of C3wt and C3KE toward different lipid groups, including glycerolipids (*e.g.* TAG and diacylglycerol, DAG), glycerophospholipids (*e.g.* PC and phosphatidylethanolamine (PE), sphingolipids (*e.g.* sphingomyelin (SPM)), and sterol lipids (*e.g.* cholesterol and cholesteryl ester) using Fat Western lipid protein overlay assay (Fig. 5). The wild type apoC-III showed robust binding to PE, PC, and SPM and, to a lesser degree, to cholesterol and DAG (Fig. 5*A*, *left*). The calculated K_A values (nmol) for PE, PC, cholesterol, DAG, and SPM were

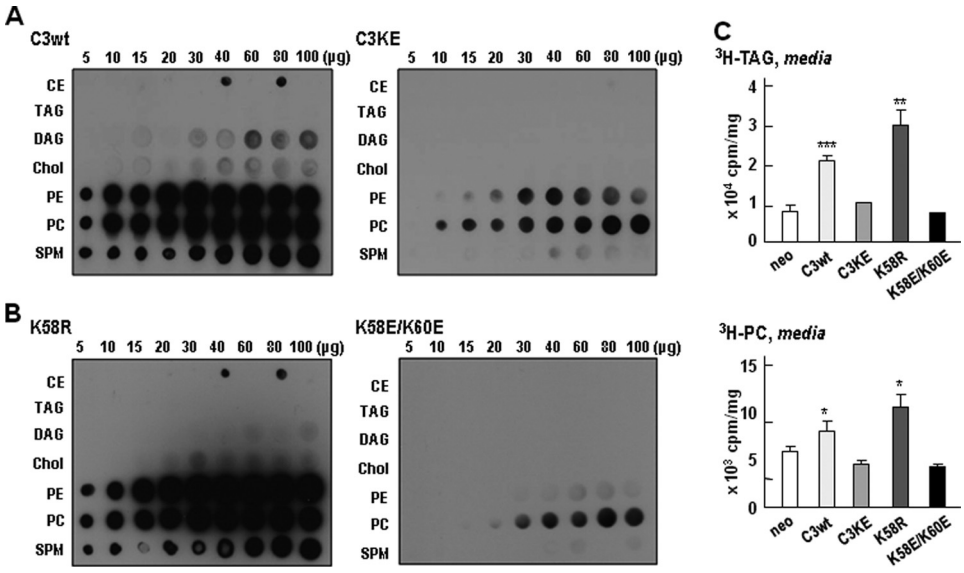

FIGURE 5. **Amphipathicity of helix 5 is important for apoC-III function.** *A* and *B*, increasing quantities (5–100 μg) of the indicated lipid groups spotted on nitrocellulose membranes were incubated with an equal amount of apoC-III collected from conditioned media of stable cell lines expressing the indicated apoC-III variants. The bound apoC-III was detected by immunoblotting, and the intensity of each spot was semiquantified by scanning densitometry (for calculating K_A values for each lipid group). *Chol*, cholesterol. *CE*, cholesteryl ester. *C*, cells (1.8×10^6 cells/60 mM dish, in triplicate) expressing the indicated apoC-III variants were labeled with [^{3}H]glycerol (5 μCi/ml) in DMEM supplemented with 20% FBS and 0.4 mM oleate, and secretion of [^{3}H]TAG and [^{3}H]PC was determined as in Fig. 1C. * $p < 0.05$; *** $p < 0.001$ (Student's *t* test of C3 variants *versus neo*; $n = 3$).

15.17, 15.60, 56.78, 62.50, and 118.80, respectively. The K_A value denotes the lipid concentrations at which apoC-III displayed half-occupation in the lipid protein overlay assay.

The C3KE mutant, at equivalent amounts of protein used, displayed drastically decreased binding toward the lipids tested (Fig. 5*A*, *right*). The calculated K_A values (nmol) for PE, PC, and SPM were 26.55, 32.01, and 71.83, respectively (lack of C3KE mutant binding to cholesterol and DAG precluded calculation of the corresponding K_A values). Thus, the binding activity to PE or PC was decreased by ~50% by the K58E mutation as compared with wild type apoC-III. Neither C3wt nor C3KE showed binding to the neutral lipids of lipoprotein core, such as TAG or cholesteryl ester. These *in vitro* data suggested strongly that the K58E mutation within helix 5 of apoC-III diminishes its binding toward the surface lipids of lipoproteins (presumably the surface lipids of LLD as well), most likely through destroyed amphipathicity of the helix.

To further test the importance of type A amphipathic configuration of helix 5, we generated two additional mutations within this region. First, Lys^{58} residue was substituted with Arg (designated K58R) to preserve the charge of the side chain. Second, both Lys^{58} and Lys^{60} residues were mutated into Glu (designated K58E/K60E) to entirely destroy the type A amphipathic helix 5 (see structure in Fig. 1*A*). Data from the lipid protein overlay assay showed, as expected, that the K58R mutation had no discernible effect on lipid binding as compared with the wild type apoC-III (Fig. 5*B*, *left*), suggesting that the charge of the side chain at position 58 is critical for lipid binding. On the other hand, the K58E/K60E mutation almost entirely abolished lipid binding of apoC-III under identical experimental conditions (Fig. 5*B*, *right*).

The effect of K58R or K58E/K60E mutation on apoC-III function in stimulating hepatic VLDL-TAG secretion was verified by metabolic labeling experiments using cells stably expressing the respective variants. Thus, although expression of the K58R mutant enhanced [^{3}H]TAG secretion as effectively as that of the wild type apoC-III, expression of the K58E/K60E mutant failed to exert an effect on [^{3}H]TAG secretion as compared with neo control cells (Fig. 5*C*). Taken together, these data highlight the importance of amphipathic helix 5 of apoC-III in mediating the formation of LLD that are utilized for VLDL assembly/secretion.

Expression of K58E Mutant Impairs DAG-to-TAG Conversion—Finally we inquired a potential effect of C3KE mutant expression on hepatic TAG biosynthesis. Metabolic labeling experiments with [^{3}H]glycerol showed that the incorporation of radiolabel into TAG was significantly decreased in C3KE cells as compared with C3wt cells (Fig. 6*A*). On the other hand, incorporation of radiolabel into PC was significantly increased in C3KE cells (Fig. 6*B*). These results indicate that the lowered incorporation into cell-associated TAG in C3KE cells was not attributable to impaired uptake of [^{3}H]glycerol. Recent studies with nonalcoholic fatty liver disease patients have implicated *APOC3* variants and hepatic DAG levels in the pathology (28, 29). Thus, we determined [^{3}H]glycerol-labeled DAG in cells expressing the recombinant human apoC-III and observed markedly increased [^{3}H]DAG during metabolic labeling in C3KE cells as compared with C3wt cells (Fig. 6*C*). We also measured secretion of [^{3}H]glycerol-labeled lipids during the labeling period. As expected, secretion of [^{3}H]TAG was markedly increased from C3wt cells as compared with C3KE cells (Fig. 6*D*), whereas secretion of [^{3}H]PC showed a significant increase at 1 h (but not 2 h) labeling time from C3KE cells (Fig. 6*E*). Secretion of [^{3}H]DAG showed no significant difference between the two cell lines (Fig. 6*F*).

We next determined whether the apparently lowered TAG synthesis in C3KE cells was attributable to impaired DAG-to-TAG conversion or else due to rapid hydrolysis of newly syn-

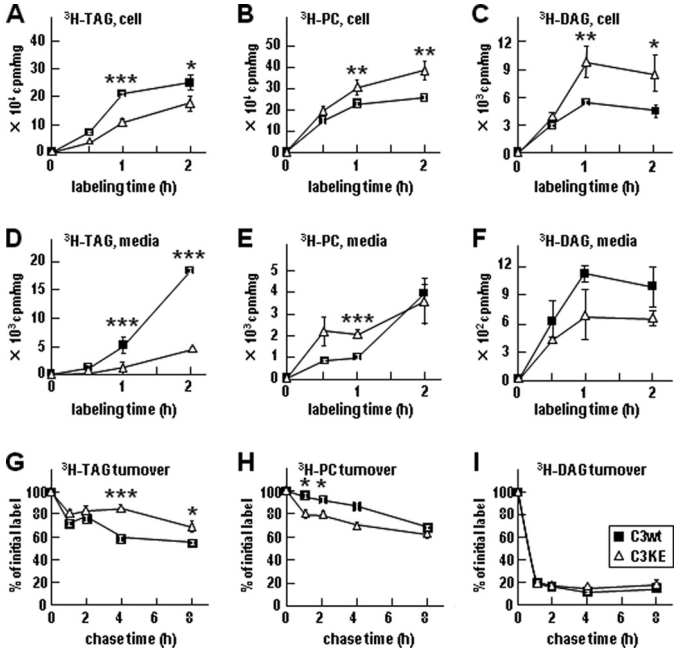

FIGURE 6. **Synthesis, secretion, and turnover of lipids in C3wt and C3KE cells.** C3wt and C3KE cells (1.8×10^6 cells/60 mM dish, in triplicate) were labeled with [^{3}H]glycerol (5 μCi/ml) for up to 2 h in DMEM containing 20% FBS and 0.4 mM oleate. Lipids were extracted from media and cells, respectively, at the end of labeling and resolved by TLC. Radioactivity associated with ^{3}H-labeled lipid was quantified by scintillation counting. *A-C*, at each time point, the radioactivity of cell-associated [^{3}H]DAG, [^{3}H]TAG, and [^{3}H]PC are shown. *D–F*, at each time point, the radioactivity of [^{3}H]DAG, [^{3}H]TAG, and [^{3}H]PC from the conditioned media is shown. *G–I*, cells were labeled with [^{3}H]glycerol (5 μCi/ml) for 1 h in DMEM supplemented with 20% FBS and 0.4 mM oleate. The cells were replaced with DMEM supplemented with 20% FBS, 0.4 mM oleate, and 40 μM triacsin C and cultured (chase) for up to 8 h. Lipids were extracted from cells and media at the indicated chase time and separated by TLC, and radioactivity associated with [^{3}H]DAG, [^{3}H]TAG, and [^{3}H]PC was quantified. The total counts (media and cell) are expressed as percent of counts at the end of initial 1 h labeling. ***, $p < 0.001$; **, $p < 0.01$; *, $p < 0.05$ (Student's *t* test of C3wt *versus* C3KE; $n = 3$).

thesized [^{3}H]TAG. To this end, we determined TAG synthesis enzyme and TAG-transfer proteins known to play a role in VLDL assembly/secretion. Quantitative RT-PCR analysis of the expression of two key genes involved in *de novo* TAG biosynthesis, namely *Lpin1* and *Dgat1/2*, showed that their expression was not diminished but, rather, augmented in C3KE cells as compared with C3wt cells (supplemental Fig. S1*A*). *In vitro* DGAT1 and DAGT2 activity assay, however, did not show a significant difference between C3wt and C3KE cells (supplemental Fig. S1*B*). Quantification of the level of newly synthesized ^{35}S-lipin-1 between C3wt and C3KE cells also did not show significant changes (supplemental Fig. S1*C*). Pulse-chase experiments showed that the turnover of [^{3}H]TAG (in the presence of triacsin C during chase) was not faster but was, rather, slower in C3KE cells as compared with that in C3wt cells (Fig. 6*G*). Thus, the decreased incorporation of ^{3}H label into TAG in C3KE cells was unlikely attributable to decreased TAG synthesis machinery or rapid turnover of newly synthesized TAG. The turnover of [^{3}H]PC (Fig. 6*H*) or [^{3}H]DAG (Fig. 6*I*) also did not show major changes between C3wt and C3KE cells.

We performed additional subcellular fractionation experiments to define mechanisms responsible for the decreased DAG-to-TAG conversion in C3KE cells. Separation of newly synthesized cell [^{3}H]DAG into microsomes and cytosol fractions revealed that in C3wt cells >90% of total [^{3}H]DAG was associated with microsomes and the remainder in cytosol. In contrast, less than 70% of total [^{3}H]DAG was present in microsomes, and the cytosolic [^{3}H]DAG accounted for 30% in C3KE cells (Fig. 7*A*). The microsome/cytosol distribution of [^{3}H]TAG (Fig. 7*B*) or [^{3}H]PC (Fig. 7*C*) between C3KE and C3wt cells was comparable. These results together indicate that the reduced [^{3}H]TAG synthesis observed in C3KE cells might be attributable to a skewed partitioning of [^{3}H]DAG toward cytosol (and thus less available for TAG synthesis), The decreased partitioning of [^{3}H]DAG into microsomes in C3KE cells was, however, unlikely to have resulted from impaired activity of MTP, because quantitative RT-PCR analysis (supplemental Fig. S1*A*) and activity assay (supplemental Fig. S1*D*) showed no decrease but, rather, an increase in the MTP mRNA and activity.

Currently, the mechanism by which expression of C3KE mutant results in decreased hepatic TAG synthesis in McA-RH7777 cells remains unclear. Histological analysis of liver samples (Fig. 8, *A–C*) and quantification of TAG mass (Fig. 8*D*) of mice infected with adv-C3wt or adv-C3KE showed no significant difference in TAG mass in the liver between the two groups.

DISCUSSION

The Lipid Binding Domain of ApoC-III—By unraveling the functional lipid-binding within the amphipathic helix 5 of human apoC-III, the current study extends our previous demonstration for an intracellular role of apoC-III in promoting hepatic VLDL assembly/secretion. Disruption of type A amphipathic configuration of helix 5 through K58E mutation results in the lack of association with LLD in the microsomes of transfected cells (Fig. 4*B*) as well as impaired binding to surface lipids *in vitro* (Fig. 5*A*). The impaired lipid binding of the mutant apoC-III was intimately linked to its inability to promote TAG-rich VLDL assembly and secretion in both transfected McA-RH7777 cells under lipid-rich conditions (Fig. 1, *D* and 1*E*) and in high fat diet-fed *apoc3*-null mice reconstituted with hepatic apoC-III expression (Fig. 3). Thus, the present cell culture and *in vivo* studies with the naturally occurring missense mutation in *APOC3* within the lipid binding domain of human apoC-III provide strong evidence for an intrahepatic cellular function of this apolipoprotein in promoting hepatic TAG-rich lipoprotein assembly/secretion.

What is the structural element within helix 5 that mediates its lipid binding to LLD? The current available structural information of human apoC-III was obtained from NMR analysis of the protein in association with SDS micelles (26). Early *in vitro* studies suggested that binding of apoC-III to phospholipids was mediated by residues 41–79 at the C terminus of the protein (15). Furthermore, site-specific mutagenesis experiments showed that two hydrophobic residues (Phe^{64} and Trp^{65}) near the carboxyl end are crucial for initiating and maintaining lipid binding of apoC-III (30). Helical wheel modeling suggests a perfect type A amphipathic α-helix for helix 5, with the nonpolar and polar faces separated by positively charged residues (*e.g.* Lys^{58}, Lys^{60}) at the interface (27). The type A amphipathic α-helix provides an optimal structural motif for binding to

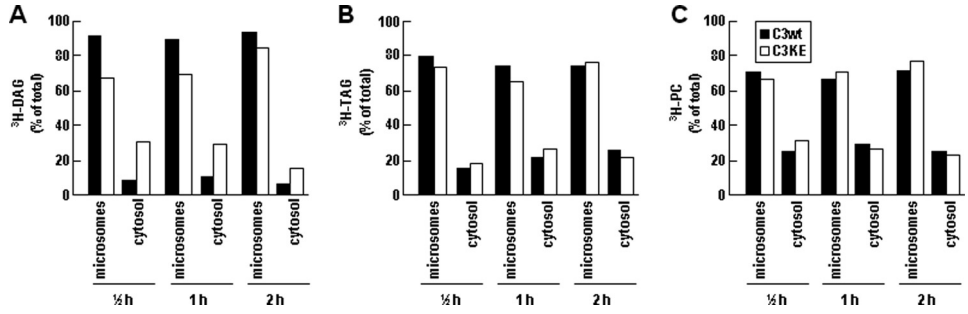

FIGURE 7. **Distribution of lipids in microsomes and cytosol are different in C3wt and C3KE cells.** The C3wt and C3KE cells (100 mm dishes, in duplicate) were labeled with [^{3}H]glycerol (20 μCi/ml) for up to 2 h in DMEM supplemented with 20% FBS and 0.4 mm oleate. The cells were harvested, and the intracellular components were separated into post-nuclear supernatant and nucleus-mitochondria (pellet) by centrifugation (1000 $\times$ *g*, 10 min, 4 °C). Post-nuclear supernatant was further separated into microsomes (pellet) and cytosol (supernatant) by ultracentrifugation (500,000 $\times$ *g*, 30 min, 4 °C). Lipids were extracted from the conditioned media as well as from all intracellular fractions and separated by TLC, and the radioactivity associated with [^{3}H]DAG (*A*), [^{3}H]TAG (*B*), and [^{3}H]PC (*C*) was quantified. The counts in microsomes and cytosol fractions were plotted as a percent of total (cellular fractions and media).

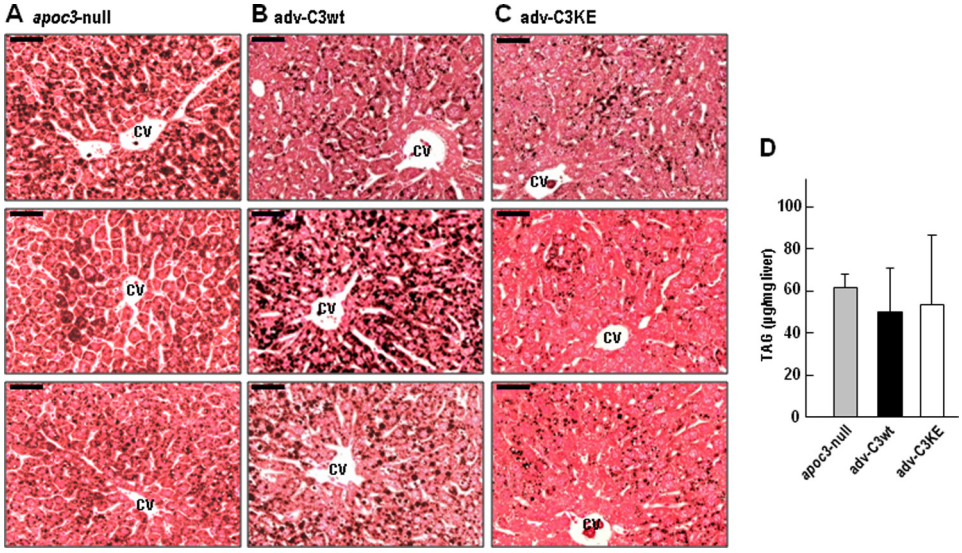

FIGURE 8. **Lipid staining of *apoc3*-null mice infected with adv-C3wt or adv-C3KE.** The experiments were performed as in Fig. 3. Two hours after P407 treatment, the mice were sacrificed, and the livers were retrieved and processed for lipid staining (*panels A–C*) and TAG mass quantification (*panel D*). *A*, liver of three control mice (*apoc3*-null mice infected with empty adenovirus vector) is shown. *B*, liver of three mice expressing C3wt is shown. *C*, liver of three mice expressing C3KE is shown. *Scale bar*, 50 μm. *CV*, central vein. *D*, TAG mass in the liver is shown. *Error bars* indicate S.D. of average TAG values of liver samples obtained from three independent mice per group.

phospholipid surface, as the positively charged patches interact with negatively charged phospholipid headgroups, whereas the hydrophobic moment of the helix buries part of the helix among the phospholipid acyl chains. The present protein lipid overlay assay has verified the specific interaction between apoC-III with amphipathic lipids, showing that the binding affinity for apoC-III toward lipids is in the order of PE > PC > SPM > cholesterol > DAG. The overlay assay also yielded insight into the effect of mutations that destroyed the type A amphipathic configuration of helix 5. For instance, K58E mutation effectively abolished binding of apoC-III with cholesterol, DAG, and SPM and significantly weakened its binding with PE and PC. However, the K58R mutation exhibited lipid binding as avidly as the wild type apoC-III, further validating amphipathic helix 5 model in which the positive charge of the side chain confers lipid binding (Fig. 5*B*). Moreover, experiments with the K58E/K60E double mutation provided further evidence for the amphipathic helix 5 model and suggested that that the two interfacial Lys residues may exert a synergistic effect on lipid binding (Fig. 5*B*).

It was reported that the heterozygote K58E carriers exhibited increased plasma HDL-cholesterol and HDL-apoA-I in the face of decreased VLDL-TAG and VLDL-apoC-III (16). The reason for this apparent hyperalphalipoproteinemia phenotype in the K58E carriers was not explained. Our cell culture experiments showed that the decreased VLDL secretion (both VLDL-apoB-100 and VLDL-TAG) from the C3KE cells was not associated with significant changes in the secretion of HDL-apoE or HDL-apoA-I (Fig. 2, *C* and *D*). Thus, the current cell culture study did not recapitulate the hyperalphalipoproteinemia phenotype in human K58E carriers. The binding of apoC-III toward HDL lipids requires further characterization.

A "Two-domain" Model for ApoC-III Action—Our studies with the naturally occurring missense mutations in *APOC3*, previously with A23T (6) and at present with K58E variants, led us to postulate a two-domain model for apoC-III action in promoting VLDL assembly/secretion under lipid-rich conditions. Although expression of both A23T and K58E displayed loss-of-function of apoC-III in promoting VLDL assembly/secretion, the underlying mechanisms for the deficiency were different.

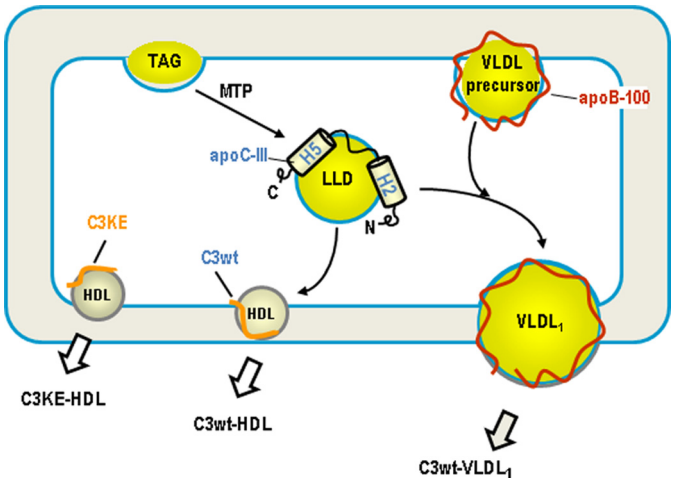

FIGURE 9. **A model for the two-domain hypothesis of apoC-III action.** The C-terminal lipid binding domain, encompassing the amphipathic α-helix 5, facilitates TAG synthesis and binding to LLD, probably through its strong interaction with glycerophospholipids. The N-terminal domain, near α-helix 2, possesses fusogenic activity in promoting fusion between LLD and VLDL precursors to form $VLDL_1$. Some apoC-III molecules remain associated with the resultant $VLDL_1$ after secretion, and the others dissociate from LLD and are secreted as HDL. The K58E mutant (*C3KE*) is unable to bind LLD or participate in $VLDL_1$ maturation and is, therefore, secreted as HDL.

Although the present study with K58E mutation indicated a deficiency in binding to surface lipids presumably surrounding the LLD, studies with the A23T mutation showed no impairment in lipid binding or LLD formation (6). We have recently verified that the A23T mutant exhibited enhanced binding to LLD in the microsomes of transfected cells and that the A23T mutation had no negative effect on apoC-III lipid binding as determined by Fat Western lipid protein overlay assay.[6] Thus, our cell culture and *in vitro* results are in agreement with previously reported thrombin cleavage studies (31) that excluded the N terminus of apoC-III being responsible for lipid binding. Remarkably, binding of A23T variant to LLD resulted in accumulation of TAG in the microsomal lumen (6). We interpreted this result as a blockage of fusion of LLD with the VLDL precursor by A23T variant and postulated that the N-terminal region of apoC-III might possess a fusogenic function in facilitating incorporation of bulk TAG (derived from LLD) into VLDL (6). On the other hand, the C-terminal α-helix 5 confers apoC-III lipid binding and promotes formation of LLD. The binding of apoC-III to LLD may represent a docking step that is the prerequisite for a subsequent fusion event. A model depicting the two-domain hypothesis for apoC-III action in promoting LLD formation and subsequent $VLDL_1$ assembly is shown in Fig. 9.

LLD Represents the TAG Precursor for $VLDL_1$ Maturation—VLDL maturation describes a process whereby the bulk TAG is incorporated, presumably in the form of metabolically active LLD. Technically, it has been challenging to determine the biosynthetic origin or the metabolic fate of LLD, because of the lack of a proper protein marker(s) for this metabolically dynamic entity. It is conceivable that formation of LLD only becomes apparent under lipid-rich conditions, through which the VLDL assembly/secretion apparatus is activated to purge excess hepatic lipid and prevent endoplasmic reticulum stress associated with lipotoxicity. In this regard, up-regulated apoC-III expression represents a hepatic defense mechanism in protecting hepatic steatosis as a consequence of the insult of excess fatty acid influx, a common feature associated with hepatic insulin resistance under diabetic conditions. The current biochemical experiments in conjunction with mass spectrometry analysis not only ascertained that apoC-III is a *bona fide* protein component of LLD but also revealed a dynamic link between the apoC-III domain structure and LLD metabolism. Thus, apoC-III is a suitable functional marker for LLD.

Notably, the impaired secretion of $VLDL_1$-TAG from cells expressing the mutant apoC-III proteins (either A23T or K58E variants) was not accompanied with TAG accumulation in transfected McA-RH7777 cells (Fig. 6*A*) or in the infected livers (Fig. 8*D*). Rather, metabolic labeling experiments with C3KE cells showed decreased [^{3}H]DAG-to-TAG conversion (Fig. 6, *A–C*), and histology studies revealed low lipid content in the liver of high fat diet-fed mice infected with the C3KE mutant. Data obtained from pulse-chase experiments with stable cell lines suggested that the decreased [^{3}H]TAG in C3KE cells was not attributable to rapid turnover of the newly synthesized TAG (Fig. 6, *G–I*). Recent studies with McA-RH7777 cells have shown that overexpression of lipin-1 (encoding phosphatidate phosphatase 1) (32) or DGAT2 (33), two key enzymes involved in the *de novo* TAG biosynthesis, resulted in increased VLDL assembly/secretion. However, expression of C3KE mutant in McA-RH7777 cells did not alter DGAT activity or lipin-1 expression (supplemental Fig. S1). Thus, the decreased TAG synthesis in C3KE cells was unlikely attributable to an altered biosynthetic enzyme machinery. Data obtained from subcellular fractionation experiments have offered some clues to a potential role of apoC-III in the partitioning DAG between the cytosol and microsomes (Fig. 7*A*). Mechanisms by which apoC-III expression facilitates the channeling of substrate DAG into TAG synthesis for VLDL assembly/secretion remain to be defined.

How apoC-III can facilitate the partitioning of lipid substrate toward microsomes as well as formation of LLD is unclear. It is known that partitioning of VLDL lipid substrates into microsomal lumen requires the activity of MTP (2–4). We have shown previously that although apoC-III could not substitute the MTP activity required for VLDL assembly/secretion, it facilitates TAG incorporation into VLDL, a process that is independent of MTP activity (14). Neither the A23T (6) nor the K58E mutation (supplemental Fig. S1) drastically altered the MTP activity in transfected cells. Thus, it is likely that the action of apoC-III is downstream of MTP-mediated TAG partitioning into microsomes (Fig. 9).

In conclusion, the present cell culture and *in vivo* mouse studies have identified the C-terminal amphipathic α-helix of apoC-III as an important functional structural element in promoting LLD formation (probably through facilitated TAG biosynthesis) and VLDL assembly/secretion. Mutations that destroy the amphipathicity of helix 5 lead to impaired formation of LLD and diminished VLDL assembly/secretion. Because active assembly and secretion of TAG-rich VLDL represents a critical component in hepatic lipid homeostasis, particularly in

[6] M. Sundaram, Y. Wang, and Z. Yao, unpublished observation.

protecting the liver from lipid overload, up-regulating apoC-III expression may represent a defense mechanism against lipotoxicity under stress conditions.

Acknowledgments—We thank Vincent Ngo for generating the K58E expression plasmid, Michele Geoffrion (University of Ottawa Heart Institute) for assistance in FPLC, Dr. Jahangir Iqbal and Dr. M. Mahmood Hussain (SUNY Downstate Medical Center) for measuring the MTP activity, and Louise B. Pelletier (University of Ottawa) for histology studies of mouse liver.

REFERENCES

1. Sundaram, M., and Yao, Z. (2010) *Nutr. Metab.* **7,** 35
2. Raabe, M., Véniant, M. M., Sullivan, M. A., Zlot, C. H., Björkegren, J., Nielsen, L. B., Wong, J. S., Hamilton, R. L., and Young, S. G. (1999) *J. Clin. Invest.* **103,** 1287–1298
3. Kulinski, A., Rustaeus, S., and Vance, J. E. (2002) *J. Biol. Chem.* **277,** 31516–31525
4. Wang, Y., Tran, K., and Yao, Z. (1999) *J. Biol. Chem.* **274,** 27793–27800
5. Wang, H., Gilham, D., and Lehner, R. (2007) *J. Biol. Chem.* **282,** 33218–33226
6. Sundaram, M., Zhong, S., Bou, Khalil, M., Zhou, H., Jiang, Z. G., Zhao, Y., Iqbal, J., Hussain, M. M., Figeys, D., Wang, Y., and Yao, Z. (2010) *J. Lipid Res.* **51,** 1524–1534
7. Jong, M. C., Hofker, M. H., and Havekes, L. M. (1999) *Arterioscler. Thromb. Vasc. Biol.* **19,** 472–484
8. Talmud, P. J., Hawe, E., Martin, S., Olivier, M., Miller, G. J., Rubin, E. M., Pennacchio, L. A., and Humphries, S. E. (2002) *Hum. Mol. Genet.* **11,** 3039–3046
9. Pollin, T. I., Damcott, C. M., Shen, H., Ott, S. H., Shelton, J., Horenstein, R. B., Post, W., McLenithan, J. C., Bielak, L. F., Peyser, P. A., Mitchell, B. D., Miller, M., O'Connell, J. R., and Shuldiner, A. R. (2008) *Science* **322,** 1702–1705
10. Ginsberg, H. N., Le, N. A., Goldberg, I. J., Gibson, J. C., Rubinstein, A., Wang-Iverson, P., Norum, R., and Brown, W. V. (1986) *J. Clin. Invest.* **78,** 1287–1295
11. Sehayek, E., and Eisenberg, S. (1991) *J. Biol. Chem.* **266,** 18259–18267
12. Zheng, C., Khoo, C., Ikewaki, K., and Sacks, F. M. (2007) *J. Lipid Res.* **48,** 1190–1203
13. Zheng, C., Khoo, C., Furtado, J., Ikewaki, K., and Sacks, F. M. (2008) *Am. J. Clin. Nutr.* **88,** 272–281
14. Sundaram, M., Zhong, S., Bou, Khalil, M., Links, P. H., Zhao, Y., Iqbal, J., Hussain, M. M., Parks, R. J., Wang, Y., and Yao, Z. (2010) *J. Lipid Res.* **51,** 150–161
15. Sparrow, J. T., Gotto, A. M., Jr., and Morrisett, J. D. (1973) *Proc. Natl. Acad. Sci. U.S.A.* **70,** 2124–2128
16. von Eckardstein, A., Holz, H., Sandkamp, M., Weng, W., Funke, H., and Assmann, G. (1991) *J. Clin. Invest.* **87,** 1724–1731
17. McLeod, R. S., Wang, Y., Wang, S., Rusiñol, A., Links, P., and Yao, Z. (1996) *J. Biol. Chem.* **271,** 18445–18455
18. Vance, D. E., Weinstein, D. B., and Steinberg, D. (1984) *Biochim. Biophys. Acta* **792,** 39–47
19. Rogers, L., Burchat, S., Gage, J., Hasu, M., Thabet, M., Willcox, L., Wilcox, L., Ramsamy, T. A., and Whitman, S. C. (2008) *Cardiovasc. Res.* **78,** 167–174
20. Zhong, S., Magnolo, A. L., Sundaram, M., Zhou, H., Yao, E. F., Di, Leo, E., Loria, P., Wang, S., Bamji-Mirza, M., Wang, L., McKnight, C. J., Figeys, D., Wang, Y., Tarugi, P., and Yao, Z. (2010) *J. Biol. Chem.* **285,** 6453–6464
21. Dowler, S., Kular, G., and Alessi, D. R. (2002) *Sci. STKE 2002,* l6
22. Cases, S., Stone, S. J., Zhou, P., Yen, E., Tow, B., Lardizabal, K. D., Voelker, T., and Farese, R. V., Jr. (2001) *J. Biol. Chem.* **276,** 38870–38876
23. Athar, H., Iqbal, J., Jiang, X. C., and Hussain, M. M. (2004) *J. Lipid Res.* **45,** 764–772
24. Chang, T. Y., Limanek, J. S., and Chang, C. C. (1981) *Anal. Biochem.* **116,** 298–302
25. Bradford, M. M. (1976) *Anal. Biochem.* **72,** 248–254
26. Gangabadage, C. S., Zdunek, J., Tessari, M., Nilsson, S., Olivecrona, G., and Wijmenga, S. S. (2008) *J. Biol. Chem.* **283,** 17416–17427
27. Segrest, J. P., De Loof, H., Dohlman, J. G., Brouillette, C. G., and Anantharamaiah, G. M. (1990) *Proteins* **8,** 103–117
28. Petersen, K. F., Dufour, S., Hariri, A., Nelson-Williams, C., Foo, J. N., Zhang, X. M., Dziura, J., Lifton, R. P., and Shulman, G. I. (2010) *N. Engl. J. Med.* **362,** 1082–1089
29. Samuel, V. T., Liu, Z. X., Wang, A., Beddow, S. A., Geisler, J. G., Kahn, M., Zhang, X. M., Monia, B. P., Bhanot, S., and Shulman, G. I. (2007) *J. Clin. Invest.* **117,** 739–745
30. Liu, H., Talmud, P. J., Lins, L., Brasseur, R., Olivecrona, G., Peelman, F., Vandekerckhove, J., Rosseneu, M., and Labeur, C. (2000) *Biochemistry* **39,** 9201–9212
31. Sparrow, J. T., Pownall, H. J., Hsu, F. J., Blumenthal, L. D., Culwell, A. R., and Gotto, A. M. (1977) *Biochemistry* **16,** 5427–5431
32. Bou Khalil, M., Sundaram, M., Zhang, H. Y., Links, P. H., Raven, J. F., Manmontri, B., Sariahmetoglu, M., Tran, K., Reue, K., Brindley, D. N., and Yao, Z. (2009) *J. Lipid Res.* **50,** 47–58
33. Stone, S. J., Levin, M. C., Zhou, P., Han, J., Walther, T. C., and Farese, R. V., Jr. (2009) *J. Biol. Chem.* **284,** 5352–5361
34. Shannon, P., Markiel, A., Ozier, O., Baliga, N. S., Wang, J. T., Ramage, D., Amin, N., Schwikowski, B., and Ideker, T. (2003) *Genome Res.* **13,** 2498–2504